
Localized states at zigzag edges of multilayer graphene and graphite steps

EDUARDO V. CASTRO¹, N. M. R. PERES² and J. M. B. LOPES DOS SANTOS¹

¹ *CFP and Departamento de Física, Faculdade de Ciências Universidade do Porto - P-4169-007 Porto, Portugal*

² *Center of Physics and Departamento de Física, Universidade do Minho - P-4710-057 Braga, Portugal*

PACS 73.20.-r – Electron states at surfaces and interfaces

PACS 73.20.At – Surface states, band structure, electron density of states

PACS 73.21.Ac – Multilayers

PACS 81.05.Uw – Carbon, diamond, graphite

Abstract. - We report the existence of zero energy surface states localized at zigzag edges of N -layer graphene. Working within the tight-binding approximation, and using the simplest nearest-neighbor model, we derive the analytic solution for the wavefunctions of these peculiar surface states. It is shown that zero energy edge states in multilayer graphene can be divided into three families: (i) states living only on a single plane, equivalent to surface states in monolayer graphene; (ii) states with finite amplitude over the two last, or the two first layers of the stack, equivalent to surface states in bilayer graphene; (iii) states with finite amplitude over three consecutive layers. Multilayer graphene edge states are shown to be robust to the inclusion of the next nearest-neighbor interlayer hopping. We generalize the edge state solution to the case of graphite steps with zigzag edges, and show that edge states measured through scanning tunneling microscopy and spectroscopy of graphite steps belong to family (i) or (ii) mentioned above, depending on the way the top layer is cut.

Introduction. – In the past few years carbon physics presented new challenges to the scientific community, increasing the list of rather unusual phenomena occurring in this life support element. On one hand, the discovery of metal free carbon-based magnetism open a new research field in fundamental physics, with possible applications in spin electronics [1–3]. On the other, the isolation of a single graphite layer – *graphene* – revealed an ultra-relativistic system full of unconventional electronic properties, and regarded with great expectation from the point of view of applications [4–6].

The origin of the observed magnetism in carbon-based materials is still under debate, but the presence of open edges seem to be an ubiquitous feature [3]. In proton bombarded graphite, which shows room temperature ferromagnetism, proton irradiation induces hydrogen-terminated edges [7, 8]. In activated carbon fibers and graphitized nanodiamond particles – known as nanographite – Curie-Weiss behavior and an enhanced paramagnetic susceptibility has been reported [2]. In these nanographites edges play a predominant role due to the built-in nano-dimension. Edges are assumed to induce π -

localized electrons due to surface (edge) states, which has been seen as a key ingredient to understand carbon’s magnetic behavior [1, 3]. Indeed, the existence of edge states localized at zigzag edges of single layer graphene, induced either by extended defects or vacancies, is now well documented and their magnetic behavior has been extensively reported [3, 9–12].

Despite the positive correlation between edge state magnetism in graphene single layer and magnetic phenomena in graphite and nanographite, strictly speaking, neither of them are a single layer of graphene. Although the inter-layer coupling is known to be very small, its effect is not negligible. To give an example, massless Dirac fermions in single layer graphene turn out to be massive in bilayer graphene [6]. This brings about the question whether edge states are robust to stacking, or in other words, whether multilayer graphene can support edge states localized on zigzag edges. Moreover, with the advent of graphene physics, also graphene multilayers (bilayer, trilayer, ...) were isolated. These graphene multilayers show interesting properties on their own [4, 6], dissimilar from their single layer constituent, and can be even more suitable for

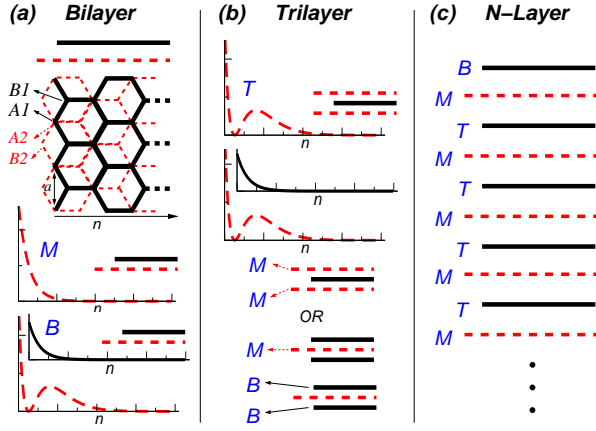


Fig. 1: (a) Side and top views of bilayer graphene, and its two families of edge states: *monolayer* (M) and *bilayer* (B); the vertical axes represent the associated charge densities (squared amplitudes). (b) *Trilayer* family of edge states (T) occurring in trilayer graphene (vertical axes represent charge densities), and all other possible edge states (in schematic view). (c) Edge states in N -layer graphene (in schematic view).

some device applications [13–15]. Therefore, the question whether multilayer graphene possesses edge state physics is of paramount importance.

In this Letter we show that zero energy states localized at zigzag edges do exist in multilayer graphene. Using the simplest first nearest-neighbor tight-binding model, we derive the analytical expression for multilayer graphene edge states and show that their number is always equal to the number of layers occurring at the edge. The effect of second nearest-neighbor interlayer hopping is considered, and the robustness of multilayer graphene edge states is shown. Finally, we generalize the edge state solution to graphite steps, where experimental evidence for edge states has been widely reported [3]. The theoretical solution given in this Letter agrees well with experimental findings. Also, we predict that edge states in graphite steps should be seen in scanning tunneling microscopy (STM) even when the step occurs underneath the first graphite layer.

Model. – We model AB -stacked multilayer graphene as shown in fig. 1(a) (for the simplest case of a bilayer), where non-interacting π -electrons are allowed to hop only between A and B sublattices. In what follows we use the terminology *balcony layers* for layers represented with dashed (red) lines, and *non-balcony* layers for those represented with full (black) lines. Without loss of generality we assume all edge atoms belong to the A sublattice. The zigzag edge breaks translational invariance along its perpendicular direction, enabling us to write an effective one-dimensional Hamiltonian for a given momentum $k \in [0, 2\pi[$ along the edge (in units of a^{-1}). The first nearest-neighbor tight-binding Hamiltonian can be writ-

ten as

$$H_k = -t \sum_i \sum_n a_{i;k,n}^\dagger (-e^{ik/2} D_k b_{i;k,n} + b_{i;k,n-1}) - t_\perp \sum_i \sum_n a_{i;k,n}^\dagger b_{i\mp 1;k,n} + \text{h.c.}, \quad (1)$$

where $a_{i;k,n}$ ($b_{i;k,n}$) is the annihilation operator at momentum k and position n in sublattice A_i (B_i), i is the layer index and $D_k = -2 \cos(k/2)$. The first term in eq. (1) describes in-plane hopping while the second term parametrizes the inter-layer coupling ($t_\perp \ll t$). The symbol \bullet indicates a sum over non-balcony layers. Afterwards we consider the second nearest-neighbor interlayer hopping between A and B sublattices, which implies an extra term in eq. (1) given by $-\gamma_3 \sum_i \sum_n b_{i;k,n}^\dagger (e^{-ik} a_{i\mp 1;k,n} - e^{-ik/2} D_k a_{i\mp 1;k,n+1}) + \text{h.c.}$, where $\gamma_3 \sim t_\perp \ll t$.

Edge states in N -layer graphene. – Multilayer graphene edge states are investigated by solving the Schrödinger equation, $H_k |\psi_k\rangle = E_k |\psi_k\rangle$. The wavefunction $|\psi_k\rangle$ is written as a linear combination of the site amplitudes along the edge's perpendicular direction, $|\psi_k\rangle = \sum_n \sum_i [\alpha_i(k, n) |a_i, k, n\rangle + \beta_i(k, n) |b_i, k, n\rangle]$, where we have introduced the one-particle states $|c_i, k, n\rangle = c_{i;k,n}^\dagger |0\rangle$, with $c_i = a_i, b_i$. In addition we require the boundary conditions $\alpha_i(k, n \rightarrow \infty) = \alpha_i(k, -1) = \beta_i(k, n \rightarrow \infty) = \beta_i(k, -1) = 0$, accounting for the existence of the edge at $n = 0$. Within our model, the Fermi energy of multilayer graphene always occurs at zero energy. Therefore, we expect zero energy edge states to have interesting physical consequences, and we set $E_k = 0$. As a result, the two sublattices become completely decoupled, and only the sublattice to which edge atoms belong can support edge states.¹ This means that we always have $\beta_i(k, n) = 0$.

It was recently shown [17] that bilayer graphene supports two types of zero energy edge states localized at zigzag edges for $2\pi/3 < k < 4\pi/3$: one type restricted to the balcony layer and coined *monolayer family*, with amplitudes equivalent to edge states in single layer graphene,

$$\alpha_2(k, n) = \alpha_2(k, 0) D_k^n e^{-i\frac{k}{2}n}; \quad (2)$$

and a new type coined *bilayer family*, with finite amplitudes over the two layers,

$$\begin{aligned} \alpha_1(k, n) &= \alpha_1(k, 0) D_k^n e^{-i\frac{k}{2}n}, \\ \alpha_2(k, n) &= -\alpha_1(k, 0) D_k^{n-1} \frac{t_\perp}{t} e^{-i\frac{k}{2}(n-1)} \left(n - \frac{D_k^2}{1 - D_k^2} \right), \end{aligned} \quad (3)$$

where the normalization constants are given by $|\alpha_2(k, 0)|^2 = 1 - D_k^2$ and $|\alpha_1(k, 0)|^2 = (1 - D_k^2)^3 / [(1 -$

¹In the ribbon geometry the two sublattices are equivalent, supporting edge states localized in opposite ribbon edges. In the semi-infinite system, only those localized in the edge sublattice survive [16, 17].

$D_k^2)^2 + t_\perp^2/t^2]$. The charge densities (squared amplitudes) associated with the two families of edge states are represented in fig. 1(a). Let us now consider a trilayer as shown in fig. 1(b), where a non-balcony layer is sandwiched between two balcony layers. Clearly, the bilayer family is not an edge state solution for this trilayer, as any finite amplitude at a non-balcony layer implies, through eq. (1), a finite amplitude over adjacent layers. We note, however, that our model ignores the coupling between next nearest-layers.² Thus, if we construct a trilayer wavefunction whose amplitudes over balcony/non-balcony layers mimic those for the bilayer family, it is guaranteed, apart from a normalization factor, that we have an edge state solution. More precisely, we arrive at a new type of edge state with finite amplitudes over three consecutive layers – *trilayer family* – whose analytic form can be written as

$$\begin{aligned}\alpha_1(k, n) &= -\alpha_2(k, 0)D_k^{n-1}\frac{t_\perp}{t}e^{-i\frac{k}{2}(n-1)}\left(n - \frac{D_k^2}{1 - D_k^2}\right), \\ \alpha_2(k, n) &= \alpha_2(k, 0)D_k^n e^{-i\frac{k}{2}n}, \\ \alpha_3(k, n) &= -\alpha_2(k, 0)D_k^{n-1}\frac{t_\perp}{t}e^{-i2(n-1)}\left(n - \frac{D_k^2}{1 - D_k^2}\right),\end{aligned}\quad (4)$$

where the normalization constant is given by $|\alpha_2(k, 0)|^2 = (1 - D_k^2)^3 / [(1 - D_k^2)^2 + 2t_\perp^2/t^2]$. The charge density (squared amplitude) associated with the trilayer family of edge states is represented in fig. 1(b).

Additionally, the trilayer we have been discussing also supports edge states of the monolayer family localized at balcony layers, as schematically shown in fig. 1(b). In fact, this is a general result. Balcony layers have an edge sublattice which is not connected through t_\perp to adjacent layers. Thus, the monolayer family is always an edge state solution in N -layer graphene. Even more generally, we can look at a balcony layer as a buffer layer. As can be seen from eq. (1), a finite amplitude over a balcony layer does not imply finite amplitudes over adjacent layers. For the trilayer shown at the bottom of fig. 1(b), where a balcony layer is sandwiched between two non-balcony layers, monolayer edge states certainly exist at the middle balcony layer. But because of the buffer layer character, also bilayer edge states are present, localized either at the two top or the two bottom layers. An immediate consequence of the buffer layer concept is the fact that the trilayer family is the most general edge state family we can have, and exists localized at any non-balcony layer and its two adjacent layers, with all other site amplitudes equal to zero. Therefore, we have three families of edge states occurring in multilayer graphene: (i) monolayer family for each balcony layer, eq. (2); (ii) bilayer family for each non-balcony layer that starts and/or ends the multilayer, eq. (3); (iii) trilayer family for each non-balcony layer sandwiched be-

tween two balcony ones, eq. (4). This is schematically represented in fig. 1(c). Note that the number of edge state families is always equal to the number of edge layers.

Effect of γ_3 . – In multilayer graphene the effect of γ_3 is of the order of t_\perp , and should be included in a consistent edge state solution. The buffer layer concept introduced previously, however, does not survive at a finite γ_3 . In order to generalize the edge state solution to the present case we use the transfer matrix technique, following ref. [17]. For bilayer graphene the transfer matrix, defined as $[\alpha_1(k, n), \alpha_2(k, n)]^T = e^{-ikn/2}\mathbf{T}(2)^n[\alpha_1(k, 0), \alpha_2(k, 0)]^T$, is given by

$$\mathbf{T}(2) = \begin{bmatrix} u & v \\ x & D_k \end{bmatrix}, \quad (5)$$

where $u = D_k(1 - \xi)$, $v = -\frac{\gamma_3}{t}e^{-ik/2}(1 - D_k^2)$, and $x = -\frac{t_\perp}{t}e^{ik/2}$, with $\xi = t_\perp\gamma_3/t^2$. The edge states are completely determined by the eigenvalues λ_\pm and eigenvectors χ^\pm of the transfer matrix. If $|\lambda_\pm| < 1$, then edge states exist and are given by $[\alpha_1(k, n), \alpha_2(k, n)]^T \propto e^{-ikn/2}\lambda_\pm^n\chi^\pm$, apart from a normalization constant. Diagonalizing eq. (5) we obtain $\lambda_\pm = D_k(1 - \xi/2) \pm \sqrt{\xi}\sqrt{D_k^2(\xi/4 - 1) + 1}$. Simple algebra shows that for λ_+ the convergence condition implies $2\cos^{-1}(\sqrt{1 + \xi}/2) < k < 2\cos^{-1}[-(1 - \xi)/2]$ or $4\pi/3 < k < 2\cos^{-1}(-\sqrt{1 + \xi}/2)$, while for λ_- it implies $2\cos^{-1}(\sqrt{1 + \xi}/2) < k < 2\pi/3$ or $2\cos^{-1}[(1 - \xi)/2] < k < 2\cos^{-1}(-\sqrt{1 + \xi}/2)$. We conclude that bilayer graphene still has two families of edge states for $\gamma_3 \neq 0$, though the k range is slightly changed when compared with the $\gamma_3 = 0$ case. In particular, we have only one family for $k \in [2\pi/3, 2\cos^{-1}[(1 - \xi)/2]]$ and $k \in [2\cos^{-1}[-(1 - \xi)/2], 4\pi/3]$, although the existence of edge states for $k < 2\pi/3$ and $k > 4\pi/3$ compensates this reduction, and we still have edge states for 1/3 of the possible k 's, as in the $\gamma_3 = 0$. As a test to what has just been said, we have numerically computed the energy spectrum for a bilayer ribbon with zigzag edges ($t_\perp = \gamma_3 = 0.2t$ and width 400 unit cells). The result is shown in fig. 2(a). Four flat bands at zero energy are clearly seen, and can be identified with the abovementioned two families of edge states, two per edge. The insets reveal the k restrictions mentioned before. In fact, the values of k that limit the existence or number of edge states coincide with the Dirac points and satellite Fermi points that arise when $\gamma_3 \neq 0$ [18], as indicated by the thin red lines (the mismatch is due to the finite width of the ribbon, and consequent edge state overlap). The transfer matrix eigenvectors can be written as $\chi^\pm = [\lambda_\pm - D_k, -\frac{t_\perp}{t}e^{ik/2}]^T$, from which we can write two families of wavefunctions, $|\psi_\pm\rangle = C_\pm \sum_{n=0}^{\infty} e^{-ikn/2}\lambda_\pm^n\chi^\pm$, where the normalization constant is given by $C_\pm = [(1 - |\lambda_\pm|^2)/(|\lambda_\pm - D_k|^2 + t_\perp^2/t^2)]^{1/2}$. Note, however, that χ^+ and χ^- are not orthogonal, implying the non-orthogonality of the two solutions $|\psi_\pm\rangle$. It is convenient to orthogonalize $|\psi_-\rangle$ with respect to $|\psi_+\rangle$, whose result can be written as $|\tilde{\psi}_-\rangle = (|\psi_-\rangle - \langle\psi_+|\psi_-\rangle|\psi_+\rangle)/(1 - |\langle\psi_+|\psi_-\rangle|^2)$, where $\langle\psi_+|\psi_-\rangle = C_+C_- (t_\perp^2/t + \xi D_k^2 - \xi)/(1 - D_k^2 + \xi)$. In

²This is a reasonable approximation since in the Slonczewski-Weiss-McClure parametrization $\gamma_2, \gamma_5 \ll t_\perp, \gamma_3$ [6].

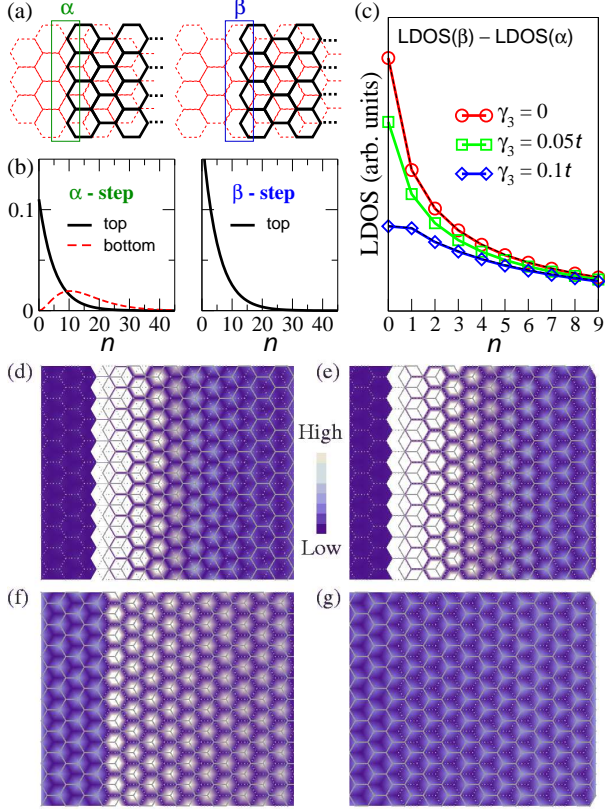


Fig. 4: (a) Possible zigzag steps on graphite's surface. (b) Charge density for edge states at α -type and β -type step-edges ($ka/2\pi = 0.35$). (c) LDOS difference between β - and α -type steps as a function of n . (d)-(e) Top layer LDOS map for α - and β -steps, respectively. (f)-(g) Underlying layer LDOS map for α - and β -steps, respectively. We set $t_{\perp} = 0.1t$.

zigzag step-edges (occurring at $n = 0$) are:

$$\begin{aligned}\alpha_{\text{top}}(k, n) &= C_k D_k^n e^{-i\frac{k}{2}n}, \\ \alpha_{\text{bottom}}(k, n) &= -C_k n D_k^{n-1} \frac{t_{\perp}}{t} e^{-i\frac{k}{2}(n-1)},\end{aligned}\quad (8)$$

for an α -type step, and

$$\alpha_{\text{top}}(k, n) = (1 - D_k^2) D_k^n e^{-i\frac{k}{2}n}, \quad (9)$$

for a β -type step, where $n \geq 0$ and the normalization constant in eq. (8) is given by $|C_k|^2 = (1 - D_k^2)^3 / [(1 - D_k^2)^2 + (1 + D_k^2)t_{\perp}^2/t^2]$. As in edge states discussed previously, the amplitudes in eqs. (8) and (9) refer to sites belonging to the same sublattice as the edge carbon atoms, while the amplitudes at the other sublattice are zero. Example charge densities for the given edge states are shown in fig. 4(b) for both the α -type and the β -type step-edges.

As can be seen from eqs. (8) and (9), or by inspection of fig. 4(b), there is an apparent asymmetry between the two families of edge states: edge states at β -type steps live only on the top layer, while at α -type steps both the top layer and the underlying layer have a finite edge state

amplitude. Consequently, we expect a similar asymmetry to be present in the LDOS peak induced by edge states at the Fermi level, which, ultimately, should be seen with STM. To better appreciate this effect, we have computed the LDOS of a generalized bilayer – bottom layer wider than the top layer – using the recursive Green's function method [30]. The calculated LDOS, which was accumulated in the range $0.01t$ near the Fermi energy, should be proportional, in the simplest approximation, to the local tunnel currents in the experimental STM images [25, 31]. In fig. 4(c) we show, for the top layer (edge sublattice), the LDOS difference between β -type and α -type terminations as we move away from the step at $n = 0$. As expected, the LDOS at β -steps is higher and extends further into the bulk, a trend that is still present for realistic values of γ_3 , as shown in fig. 4(c). This behavior agrees with STM results, where two types of edge states with different penetration depths have been seen [26]. Edge states with reduced penetration depth have been observed at α -type steps, whereas at β -type steps the edge states extend further into the bulk, as we have obtained here for the top layer component. However, right at the edge, the STM intensity has been found to be higher at α -steps than β -steps [26]. According to our analytical result the opposite should be seen. This discrepancy is most probably due to edge state admixture, as experimentally both α -type and β -type steps coexist on the same step-edge.

In fig. 4(d) and 4(e) we show the top layer LDOS map for α - and β -steps, respectively. The former presents not only a reduced penetration depth, as previously discussed, but also higher intensity at sites connected to the underlying layer through t_{\perp} , as opposed to standard LDOS maps on the surface of bilayer graphene and graphite. This behavior is characteristic of edge states at α -type steps, as given by eq. (8). fig. 4(f) and 4(g) show the underlying layer LDOS map for α - and β -steps, respectively. As edge states at α -steps [eq. (8)] have a finite amplitude over the underlying layer, the LDOS map for this layer shows an increased intensity at and near the step [fig. 4(f)], although the lattice discontinuity only exists at the other layer. As a consequence, we expect α -steps to be detected in STM experiments even when they occur underneath the top layer. This feature is not seen in β -type steps [fig. 4(g)].

Conclusions. – We have demonstrated the existence of zero energy states localized at zigzag edges of multilayer graphene and graphite steps. Stability to the presence of interlayer hopping γ_3 has been shown. The electron-hole symmetry breaking terms γ_4 (interlayer) and t' (inplane) are expected to induce edge state dispersion, but not to qualitatively modify the present results [32, 33]. It should be noted that only perfect zigzag edges have been discussed here. However, we expect edge state properties to be present in multilayer graphene and graphite steps even for irregular edges, as long as some zigzag units are present, as recently demonstrated for single layer graphene [34, 35]. On the other hand, zigzag edges have been re-

cently observed in epitaxial graphene monolayer [36], providing the first indication that edge shape can be a controllable parameter in the future. Our findings are relevant in the context of carbon based magnetism, where edge states seem to play an important role [1,3], and also in the context of graphene physics, where the reported self-doping in monolayer graphene [36] and suppression of conductance fluctuations near the neutrality point in bilayer and trilayer graphene [37] can be seen as edge states driven effects.

* * *

E.V.C., N.M.R.P., and J.M.B.L.S. acknowledge financial support from POCI 2010 via project PTDC/FIS/64404/2006.

REFERENCES

- [1] MAKAROVA T. and PALACIO F., (Editors) *Carbon Based Magnetism* (Elsevier, Amsterdam) 2006.
- [2] ENOKI T. and KOBAYASHI Y., *J. Mater. Chem.* , **15** (2005) 3999 .
- [3] ENOKI T., KOBAYASHI Y. and FUKUI K., *Int. Rev. Phys. Chem.* , **26** (2007) 609.
- [4] GEIM A. K. and NOVOSELOV K. S., *Nat. Mater.* , **6** (2007) 183.
- [5] KATSNELSON M. I., *Mater. Today* , **10** (2007) 20.
- [6] CASTRO NETO A. H., GUINEA F., PERES N. M. R., NOVOSELOV K. S. and GEIM A. K., *The electronic properties of graphene* arXiv:0709.1163 (to appear in *Rev. Mod. Phys.*).
- [7] KOPELEVICH Y. and ESQUINAZI P., *J. Low Temp. Phys.* , **146** (2007) 629.
- [8] OHLDAG H., TYLISZCZAK T., HÖHNE R., SPEMANN D., ESQUINAZI P., UNGUREANU M. and BUTZ T., *Phys. Rev. Lett.* , **98** (2007) 187204.
- [9] PEREIRA V. M., GUINEA F., LOPES DOS SANTOS J. M. B., PERES N. M. R. and CASTRO NETO A. H., *Phys. Rev. Lett.* , **96** (2006) 036801.
- [10] WAKABAYASHI K., *Electronic and magnetic properties of nanographite in Carbon Based Magnetism*, edited by MAKAROVA T. and PALACIO F., (Elsevier, Amsterdam) 2006 Ch. 12 pp. 279–304.
- [11] LEHTINEN P. O., FOSTER A. S., MA Y., KRASHENINNIKOV A. V. and NIEMINEN R. M., *Phys. Rev. Lett.* , **93** (2004) 187202.
- [12] SON Y.-W., COHEN M. L. and LOUIE S. G., *Nature* , **444** (2006) 347.
- [13] CASTRO E. V., NOVOSELOV K. S., MOROZOV S. V., PERES N. M. R., LOPES DOS SANTOS J. M. B., NILSSON J., GUINEA F., GEIM A. K. and CASTRO NETO A. H., *Phys. Rev. Lett.* , **99** (2007) 216802.
- [14] OOSTINGA J. B., HEERSCHKE H. B., LIU X., MORPURGO A. F. and VANDERSYPEN L. M. K., *Nat. Mater.* , **7** (2008) 151 .
- [15] LIN Y.-M. and AVOURIS P., *Nano Lett.* , **8** (2008) 2119.
- [16] WAKABAYASHI K., FUJITA M., AJIKI H. and SIGRIST M., *Phys. Rev. B* , **59** (1999) 8271.
- [17] CASTRO E. V., PERES N. M. R., LOPES DOS SANTOS J. M. B., CASTRO NETO A. H. and GUINEA F., *Phys. Rev. Lett.* , **100** (2008) 026802.
- [18] MCCANN E. and FAL'KO V. I., *Phys. Rev. Lett.* , **96** (2006) 086805.
- [19] LEE H., SON Y.-W., PARK N., HAN S. and YU J., *Phys. Rev. B* , **72** (2005) 174431.
- [20] SAHU B., MIN H., MACDONALD A. H. and BANERJEE S. K., *Phys. Rev. B* , **78** (2008) 045404.
- [21] MIYAMOTO Y., NAKADA K. and FUJITA M., *Phys. Rev. B* , **59** (1999) 9858 .
- [22] KLUSEK Z., WAQAR Z., DENISOV E. A., KOMPANIETS T. N., MAKARENKO I. V., TITKOV A. N. and BHATTI A. S., *Appl. Surf. Sci.* , **508** (2000) 161.
- [23] NIIMI Y., MATSUI T., KAMBARA H., TAGAMI K., TSUKADA M. and FUKUYAMA H., *Appl. Surf. Sci.* , **241** (2005) 43.
- [24] KOBAYASHI Y., ICHI FUKUI K., ENOKI T., KUSAKABE K. and KABURAGI Y., *Phys. Rev. B* , **71** (2005) 193406.
- [25] NIIMI Y., MATSUI T., KAMBARA H., TAGAMI K., TSUKADA M. and FUKUYAMA H., *Phys. Rev. B* , **73** (2006) 085421.
- [26] KOBAYASHI Y., FUKUI K., ENOKI T. and KUSAKABE K., *Phys. Rev. B* , **73** (2006) 125415.
- [27] BANERJEE S., SARDAR M., GAYATHRI N., TYAGI A. K. and RAJ B., *Appl. Phys. Lett.* , **88** (2006) 062111.
- [28] SUGAWARA K., SATO T., SOUMA S., TAKAHASHI T. and SUEMATSU H., *Phys. Rev. B* , **73** (2006) 045124.
- [29] FUJITA M., WAKABAYASHI K., NAKADA K. and KUSAKABE K., *J. Phys. Soc. Jpn.* , **65** (1996) 1920.
- [30] HAYDOCK R., *The recursive solution of the schrödinger equation in Solid State Physics*, edited by EHRENREICH H., SEITZ F. and TURNBULL D., Vol. 35 (Academic Press, New York) 1980 p. 215.
- [31] TERSOFF J. and HAMANN D. R., *Phys. Rev. B* , **31** (1985) 805 .
- [32] PERES N. M. R., GUINEA F. and CASTRO NETO A. H., *Phys. Rev. B* , **73** (2006) 125411.
- [33] SASAKI K., MURAKAMI S. and SAITO R., *Appl. Phys. Lett.* , **88** (2006) 113110.
- [34] KUMAZAKI H. and HIRASHIMA D. S., *J. Phys. Soc. Jpn.* , **77** (2008) 044705.
- [35] BHOWMICK S. and SHENOY V. B., *J. Chem. Phys.* , **128** (2008) 244717.
- [36] DE PARGA A. L. V., CALLEJA F., BORCA B., JR M. C. G. P., HINAREJO J. J., GUINEA F. and MIRANDA R., *Phys. Rev. Lett.* , **100** (2008) 056807.
- [37] STALEY N. E., PULS C. and LIU Y., *Phys. Rev. B* , **77** (2008) 155429.